Full-Wave Characterization of a Through Hole Via in Multi-Layered Packaging

Show-Gwo Hsu and Ruey-Beei Wu

Abstract—**A full-wave analysis is presented for the propagation characteristics of a through hole via connecting two semi-infinitely long transmission lines in multi-layered packaging environment. The current distribution on the via and a section of transmission line is solved under the thin wire approximation by the moment method and the scattering parameters are extracted by the matrix pencil method. The Green's function in multilayer packaging environment is derived by applying the image theory and evaluated by the help of the Poisson summation formula. Numerical results are included to investigate the frequency-dependent propagation characteristics for via structures with various geometrical parameters, e.g., the via height, wire diameter, and distance between two ground planes. The excitation of the radial waves due to the current distribution on the via is also discussed in detail.**

I. Introduction

TO COPE with the ever increasing circuit demand of higher density and faster operating speed, the multi-layer modules have become the indispensable trend of the present high-performance packaging systems [1]. In the multi-layer modules, there are striplines and/or microstrip lines for the signal transmission as well as the vias for the connections between signal lines at different layers [2]. Unlike the microstrip lines or striplines, the vias do not have parallel ground plane(s) to support well-guided electromagnetic waves. As a result, the signals propagating through the vias or the transition between vias and signal lines will very likely to suffer from the signal reflection and energy loss, either radiating into the free space or exciting the radial waves between two metallization planes.

At lower frequencies, the discontinuity that occurs as a result of the via would physically introduce excess energy storage in the electric and magnetic fields, which can be modeled by lumped capacitance and inductance, respectively. The equivalent circuits for some basic via structures have been presented by several investigators on the basis of quasistatic analysis. Wu *et al.* applied the idea of partial equivalent element circuit (PEEC), originally developed by Ruehli [3], to find the capacitances of vias in mesh plane environment [4] and the inductances of vias in three-dimensional packaging structures [5]. Wang *et al.* developed simplified formulation for several specific via structures, e.g., a via connecting two semi-infinitely long transmission lines above a ground plane [6] or penetrating through a hole in a ground plane [7]. Others investigated the effects on the equivalent capacitance due to the presence of the substrate [8] and the finite thickness of the ground plate [9].

As the operating frequencies become ever higher, strong interaction between the stored electrical and magnetic energy near discontinuity results in significant electromagnetic wave radiation. The full-wave techniques should be resorted to properly predict the characteristics of vias. Becker *et al.* employed the finite-difference time-domain (FD-TD) method to investigate a through hole via in a metallic box environment [10]. Sorrentino *et al.* applied the mode-matching method to deal with a grounding via structure that is enclosed by a metallic box to form a metallic waveguide [11]. Hsu *et al.* combined the matrix pencil approach with the moment method to extract both the frequency-dependent propagation characteristics and radiation effects of a via penetrating through a ground plane [12]. Also, Zheng *et al.* constructed a Norton equivalent circuit to investigate the electromagnetic coupling through a via with one end in the free space and the other connecting to a transmission line [13].

The adjacent two conducting plates in the multilayer packaging environment form a radial waveguide. The current on the vertical via will excite electromagnetic waves propagating inside the radial waveguide, so called the radial waves. Since the radial dimension of the conducting plates is much larger than the via height, the occurrence of the radial waves is noticeable even in low frequencies and have attracted researchers' attentions in the recent years. Fang *et al.* mentioned that the characteristic impedance of the radial wave rather than the via inductance should be considered in the simulation of the power noise between two conducting plates shorted by a vertical via [14]. Jong *et al.* discussed the effects of the radial waves due to the transient source at a vertical via which may be positioned at corner, edge, or interior of the conducting plates [15].

II. Statement of the Problem

The via in multilayered structures may pass through several conducting plates to connect two semi-infinitely long transmission lines. The whole via can be divided into two basic constitutive parts, one for the via vertically passing through two consecutive conducting plates and the other for the via penetrating a hole in a conducting plate to connect a semi-infinitely long transmission line in another layer. The structure for the first part has the cylindrical symmetry and can be reduced to a two-dimensional problem. Gu *et al.* have considered this problem and derived an analytical expression

Manuscript received June 8, 1994; revised September 27, 1994. This work was supported in part by the National Science Council, R. O. C., under the Grant NSC-84-2215-E-002-030.

The authors are with the Department of Electrical Engineering, National Taiwan University, Taipei, Taiwan, R.O.C.

IEEE Log Number 9410330.

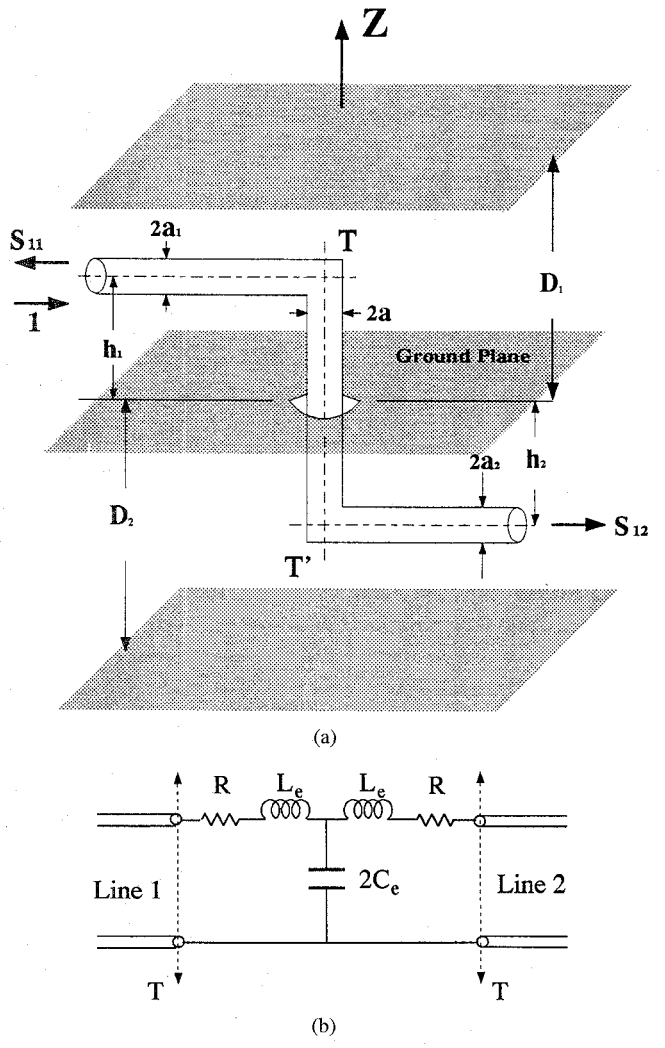

Fig. 1. (a) A typical through hole via structure in multi-layered packaging and (b) its equivalent circuit.

for the equivalent network model of the via [16]. Hence, this paper will focus on the analysis of the second part, which is a three-dimensional problem due to the presence of the transmission line.

Consider a via penetrating a hole in a ground plane to connect two semi-infinitely long transmission lines in different layers between two parallel plates, as shown in Fig. 1(a). To simplify the analysis, the transmission lines are assumed to be of circular cross-section and of radii a_1 and a_2. They have the heights of h_1 and h_2 as measured from the center plate, both lying between two parallel plates of separations D_1 and D_2,, respectively. The via and hole are also assumed to be circular and have the radii of a and b, respectively.

Also shown in the figure is a TEM wave of unit magnitude incident from the left of upper transmission line. It is desirable to find the amplitude of the reflected wave in the upper transmission line, i.e., S_{11}, and that of the transmitted wave in the lower transmission line, i.e., S_{12}. In addition, the region between each two adjacent parallel plates forms a radial waveguide structure for the vertical via. The excited radial waves due to the via will interact with the TEM waves along the transmission lines and exhibit more complicated mode transition mechanism. Fig. 1(b) shows the equivalent circuit of the via. It includes not only the inductance and capacitance to model the excessively stored magnetic and electric energy, but also the resistance to account for the transition mechanism to radial waves.

To facilitate the network formulization, assume that TEM waves of amplitudes A_1 and A_2 are incident from the upper and lower transmission lines, respectively. It is of interest to calculate the amplitudes B_1 and B_2 of the reflected TEM waves on the two transmission lines due to the presence of the via and the modal amplitudes of the resultant radial waves. A matrix-penciled moment method has been developed to deal with the same structure in the absence of upper and lower parallel plates [12]. The analysis follows a similar procedure and will be briefly described here. Note that the method is not limited to transmission lines of circular cross-section. It can apply to transmission lines of general type as well, but usually requiring greater computational effort.

The through hole via problem can be simplified by employing the equivalence principle to divide the original structure into two subregions shown in Fig. 2(a). The via hole is covered by a perfect conductor and surrounded on both sides by opposite equivalent magnetic currents $\vec{M}$ and $-\vec{M}$ satisfying

$$\vec{M} = -\hat{n} \times \vec{E}_t = -\frac{V_0}{\rho \ln(b/a)}\hat{\phi} \tag{1}$$

where $\hat{n} = \hat{z}$ is the unit vector normal to the ground plane, $\vec{E}_t$ is the tangential electric field on the aperture, $\hat{\phi}$ is the unit vector along the azimuthal direction of the hole, ρ is the radial distance from the via axis, and V_0 is the voltage across the via hole. Note that the magnetic current can also be modeled as a delta gap generator of voltage drop V_0 between the end of via and the center ground plane, if the radius of the via hole is very small [13].

In each subregion, the propagation characteristics can be attributed to the incident TEM wave of amplitude A_i and the voltage V_0. Hence, the problem can be further decomposed into two parts. One is an antenna problem shown in Fig. 2(b), where a wire antenna is bent into a transmission line. The other is a short circuit problem shown in Fig. 2(c), where the transmission line is shorted to the ground plane by the via.

By the superposition principle, the amplitude B_i of the reflected wave and the current $I_i(0)$ at the via end can be written as

$$\begin{bmatrix} B_i \\ I_i(0) \end{bmatrix} = \begin{bmatrix} \Gamma_{sc,i} & T_{ant,i} \\ I_{sc,i} & Y_{ant,i} \end{bmatrix} \begin{bmatrix} A_i \\ V_0 \end{bmatrix} \quad (i = 1, 2) \tag{2}$$

where the index $i = 1$ and 2 represent the quantities in the upper and lower spaces, respectively. Note that the current at the end $I_1(0) = -I_2(0)$, as evident from Fig. 2(a). Given the amplitudes A_1 and A_2 of the incident waves, $I_1(0)$ and $I_2(0)$ in (2) may be eliminated to yield the voltage drop

$$V_0 = -(I_{sc,1} \cdot A_1 + I_{sc,2} \cdot A_2)/Y_{ant}^t \tag{3}$$

where $Y_{ant}^t = Y_{ant,1} + Y_{ant,2}$ is the total input admittance of the associated antenna problems. By substituting (3) into (2), the amplitudes of the reflected TEM waves can be expressed

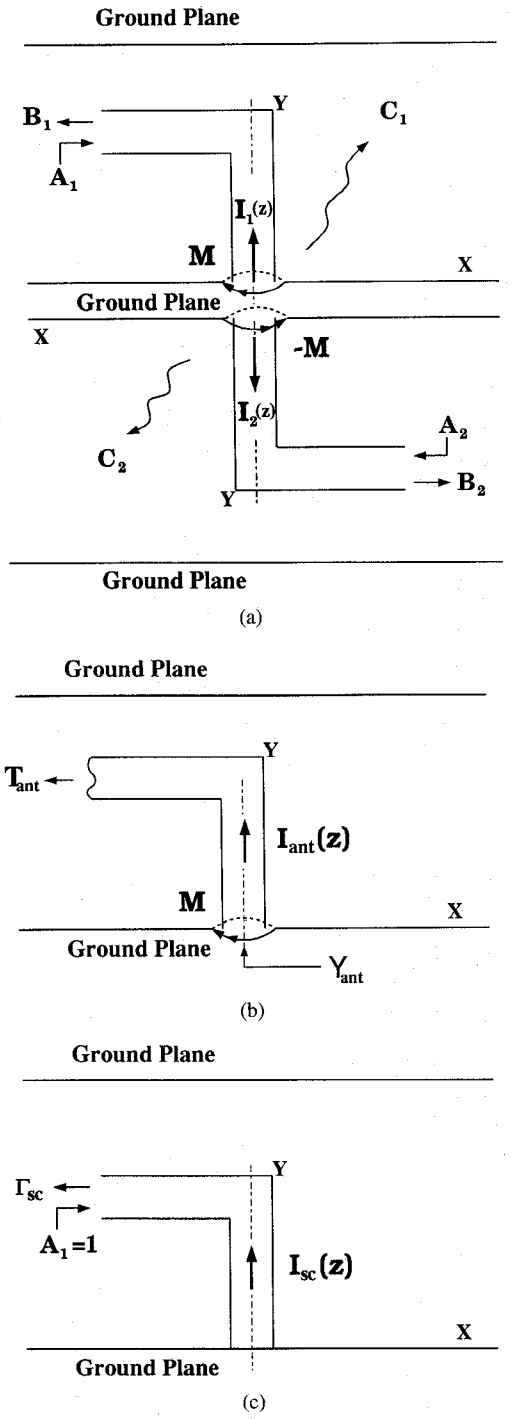

Fig. 2. (a) The equivalent structure, (b) associated wire antenna problem, and (c) short-circuit problem.

in terms of the incident wave amplitudes by

$$\begin{bmatrix} B_1 \\ B_2 \end{bmatrix} = \begin{bmatrix} S_{11} & S_{12} \\ S_{21} & S_{22} \end{bmatrix} \begin{bmatrix} A_1 \\ A_2 \end{bmatrix} \tag{4}$$

where the scattering parameters satisfy

$$\begin{aligned} S_{ii} &= \Gamma_{sc,\,i} - I_{sc,\,i} \cdot T_{ant,\,i}/Y^t_{ant} \quad (i = 1,\, 2) \\ S_{12} &= S_{21} = -I_{sc,\,2} \cdot T_{ant,\,1}/Y^t_{ant}. \end{aligned} \tag{5}$$

III. Green's Function

Only the original structure in a half space is of concern for either the short circuit problem or the wire antenna problem. Let the semi-infinitely long transmission line be truncated to a certain length L. By the image theory, the two ground planes can be replaced by both including the infinite images of the via and transmission line and imposing a delta gap voltage of $2V_0$ on each via hole, as shown in Fig. 3. As far as the discontinuity is concerned, its scattering parameters can be extracted successfully by the matrix pencil approach without requiring a matched load at the truncated end of the transmission line [12]. An ideal current source of I_0 is simply imposed there for the sake of convenience. Under the thin wire approximation, the unknown current distribution on the curved wire satisfies the integral equation [17]

$$\int \left(\frac{\partial^2}{\partial s \partial s'} - k^2 \right) G(s,\, s') I(s')\, ds' = j\omega\epsilon \hat{s} \cdot \vec{E}^i(s). \tag{6}$$

Here, s is the arc-length measured from the truncated end of the transmission line; $\hat{s}$ is the unit vector tangential to the wire at s; and k is the free space wavenumber. Taking all the infinite images into account, the Green's function in the multi-layer environment can be written as

$$\begin{aligned} G(s,\, s') &= \sum_{l=-\infty}^{\infty} \frac{e^{-jkR_l}}{4\pi R_l}; \\ R_l &= \sqrt{(\rho - \rho')^2 + (z - z' + 2lD)^2}. \end{aligned} \tag{7}$$

The series in (7) is slowly convergent since the terms are proportional to $1/l$ for large l. To facilitate the numerical calculation, Poisson summation formula

$$\sum_{l=-\infty}^{\infty} f(l) = \sum_{l=-\infty}^{\infty} F(2l\pi) \tag{8}$$

can be applied to evaluate the series, where $F(\omega)$ is the Fourier transform of $f(t)$. The function $F(\omega)$ is readily available, based on the identity [18]

$$\begin{aligned} &2 \int_0^{\infty} \frac{e^{-j\beta\sqrt{t^2+\alpha^2}}}{\sqrt{t^2+\alpha^2}} \cos \omega t\, dt \\ &\quad = \begin{cases} 2K_0(\alpha\sqrt{\omega^2 - \beta^2}) & \text{if } \omega > \beta > 0 \\ -j\pi H_0^{(2)}(\alpha\sqrt{\beta^2 - \omega^2}) & \text{if } \beta > \omega > 0 \end{cases} \end{aligned} \tag{9}$$

where $H_0^{(2)}$ and K_0 are the Hankel function and modified Bessel functions, respectively, of the second kind. Then, in common case that $k < \pi/D$, the Green's function can be rewritten as

$$\begin{aligned} G(s,\, s') = &\frac{1}{2\pi D} \sum_{l=1}^{\infty} K_0\left(\sqrt{\left(\frac{l\pi}{D}\right)^2 - k^2} \Delta\rho \right) \\ &\cdot \cos\left(l\pi \Delta z/D\right) - \frac{j}{8D} H_0^{(2)}(k\Delta\rho) \end{aligned} \tag{10}$$

where $\Delta\rho = |\rho - \rho'|$ and $\Delta z = |z - z'|$. Note that the series in (10) converges very fast since K_0 is exponentially decaying with the rate $e^{-l\pi\Delta\rho/D}$ for large l.

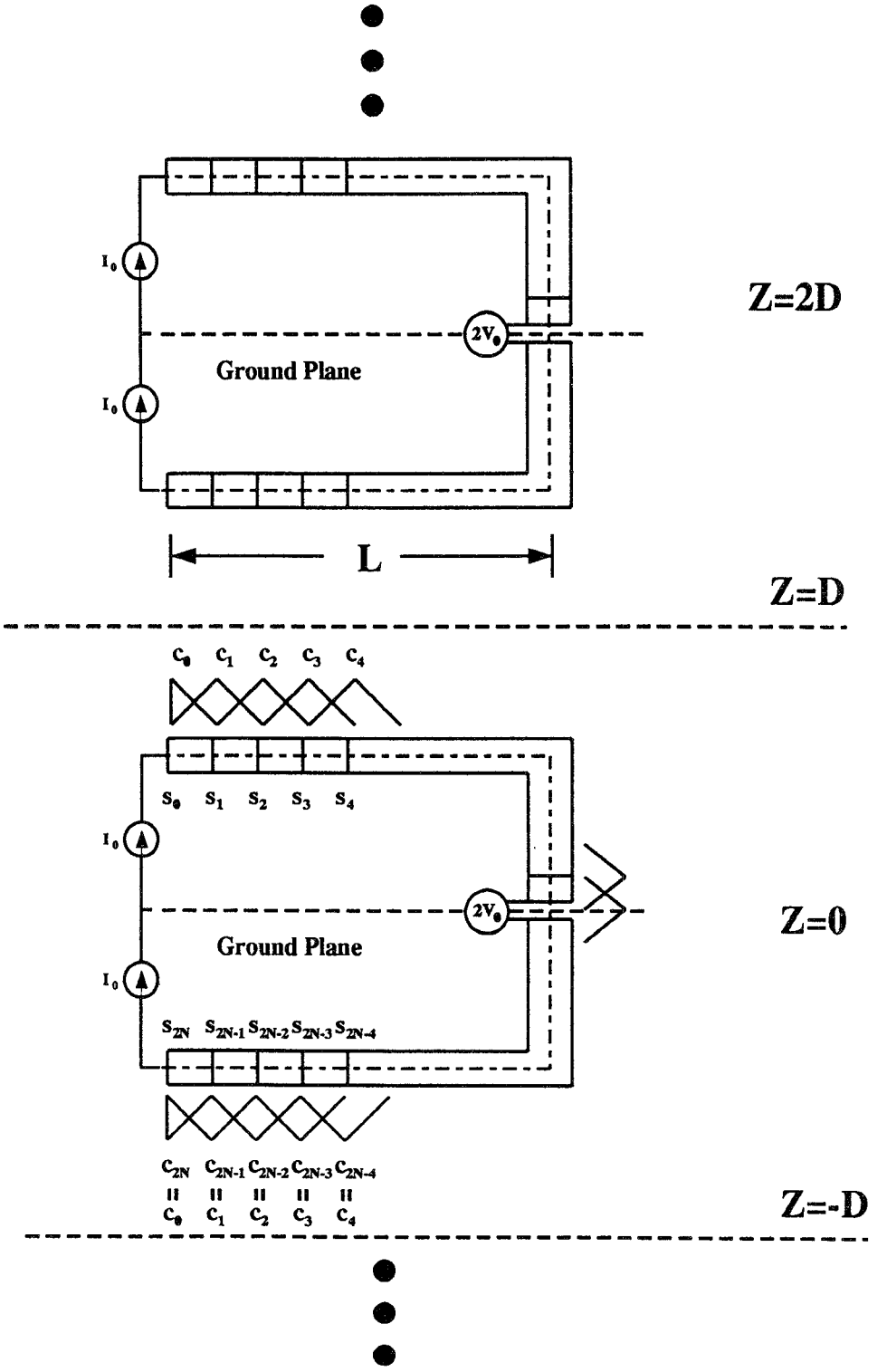

Fig. 3. The infinite imaged structure and the piecewise triangular basis functions for the current distribution on the via and a section of transmission line.

IV. Solution Procedure

Given the Green's function, the integral equation (6) can be solved by applying the moment method [17]. As shown in Fig. 3, the wire is subdivided into segments and the unknown current is expressed in terms of the piecewise triangular basis functions by

$$I(s) = \sum_{n=0}^{2N} c_n f_n(s) \tag{11}$$

where c_n denotes the current at the nth sampling point $\vec{s}_n$. Note that $c_n = c_{2N-n}$ due to the structural symmetry. Sub-

stituting (11) into (6) and applying the Galerkin's procedure yields a matrix of equation for unknown coefficients c_n's. By assuming the impressed voltage V_0 and the current source $c_0 = c_{2N} = I_0$, the matrix equation can become solved to obtain the current distribution on the via and the section of transmission line.

The desired scattering parameters can be extracted from the current distribution under suitable excitations. The analysis procedure can be briefly described as follows.

First, the short-circuit problem shown in Fig. 2(c) is considered by assuming a zero voltage drop $V_0 = 0$ and a unit ideal current source at the truncated end ($I_0 = 1$). The current distribution can be solved from (6) and the incident and reflected components, A_1 and B_1, of the TEM waves in the transmission line can be extracted by the matrix pencil method [19]. For the sake of normalization by power, the two components are multiplied by $\sqrt{Z_{0,1}/2}$ and $-\sqrt{Z_{0,1}/2}$, respectively, to give the desired modal amplitudes A_1 and B_1. Here

$$Z_{0,1} = \frac{\eta}{2\pi} \ln\left(\frac{2D_1}{a_1\pi} \sin\left(\frac{h_1}{D_1}\pi\right)\right) \tag{12}$$

is the characteristic impedance of the transmission line and $\eta = \sqrt{\mu/\epsilon}$ is the intrinsic impedance in the upper subregion. Let $I_{sc,1}(z)$ denote the current distribution at the upper via in the short circuit problem due to an incident wave of unit amplitude. The current distribution obtained under the present excitation will be $I_{sc,1}(z) \cdot A_1$. Given the extracted amplitude A_1, the short circuit current distribution $I_{sc,1}(z)$ can be found. Meanwhile, the parameters in (2) can be given by $\Gamma_{sc,1} = B_1/A_1$ and $I_{sc,1} = I_{sc,1}(0)$.

Secondly, the wire antenna problem shown in Fig. 2(b) requires solving by assuming a unit voltage drop ($V_0 = 1$). Having no suitable model for the matched boundary condition at the truncated end, an ideal open circuit is instead enforced there, i.e., $I_0 = 0$. Following a similar procedure, the via current $I_1(z)$ can be obtained and the amplitudes A_1 and B_1 be extracted. Let $I_{ant,1}(z)$ denote the current distribution on the upper via in the wire antenna problem with unit impressed voltage, but in the absence of incident wave. By the superposition principle, the via current $I_1(z)$ satisfies

$$I_1(z) = I_{sc,1}(z) \cdot A_1 + I_{ant,1}(z) \cdot V_0. \tag{13}$$

Note that $V_0 = 1$ under the present excitation and $I_{sc,1}(z)$ is readily available from the previous solution of the short-circuit problem. Given the extracted amplitude A_1, $I_{ant,1}(z)$ can be found from (13) accordingly. The desired parameters in (2) are now given by $Y_{ant,1} = I_{ant,1}(0)$ and $T_{ant,1} = B_1 - \Gamma_{sc,1} \cdot A_1$ where $\Gamma_{sc,1}$ has already been obtained in the previous problem.

Similar procedure can be performed for the structure in the lower subregion to obtain the corresponding parameters $\Gamma_{sc,2}$, $I_{sc,2}$, $Y_{ant,2}$ and $T_{ant,2}$ as well as the current distributions $I_{sc,2}(z)$ and $I_{ant,2}(z)$. By combining all these parameters in the two subregions, the scattering parameters for the original structure can be obtained from (5). The current on the upper via $I_1(z)$, and similarly for $I_2(z)$ on the lower via, can be found from (13) under incident TEM waves of arbitrary amplitudes A_1 and A_2, since the voltage drop across the via hole V_0 is readily available from (3).

V. Excitation of Radial Waves

When the operating frequency is lower than $1/(2D\sqrt{\mu\epsilon})$, i.e., $kD \leq \pi$, only the fundamental TM_0^z mode can propagate in the radial waveguide formed by two adjacent parallel plates with separation D. The TM_0^z mode is excited solely from the z-directed current on the via, which is assumed to be free of azimuthal dependence. Without loss of generality, consider the upper radial waveguide formed by the upper plate and the center ground plane in Fig. 2(a). The vector potential and the electromagnetic field of the TM_0^z can be written as [20]

$$\begin{aligned} \vec{A}_{\mathrm{TM}_0} &= \hat{z} j \frac{p_1}{\omega} H_0^{(2)}(k\rho) \\ \vec{E}_{\mathrm{TM}_0} &= \hat{z} p_1 H_0^{(2)}(k\rho) \\ \vec{H}_{\mathrm{TM}_0} &= \hat{\phi} j \frac{p_1}{\eta} H_1^{(2)}(k\rho) \end{aligned} \tag{14}$$

where the factor $p_1 = \sqrt{\omega\mu/2D_1}$ is chosen such that the mode carries a unit power, i.e.

$$\tfrac{1}{2} \int_S \mathrm{Re}\,[\vec{E}_{\mathrm{TM}_0} \times \vec{H}^*_{\mathrm{TM}_0}] \cdot \hat{\rho}\, dS = 1.$$

The vector potential in the upper subregion can be found from the current distribution on the via and the transmission line. Its z-component is given by

$$A_z(\vec{\rho}) = \mu \int G(\vec{\rho}, z') I_1(z')\, dz' \tag{15}$$

where $I_1(z')$ is the current on the via and its image inside one period shown in Fig. 3. In the far zone ($\rho \to \infty$), only the last term in (10) of the Green's function need be considered and consequently

$$\lim_{\rho\to\infty} A_z(\vec{\rho}) = -\frac{\mu h_1}{4D_1} j\overline{I}_1 H_0^{(2)}(k\rho) \tag{16}$$

where

$$\overline{I}_1 = \frac{1}{h_1} \int_0^{h_1} I_1(z')\, dz'$$

is the average current on the via. Comparing (16) with the vector potential of TM_0^z mode in (14), the modal amplitude of the TM_0^z radial wave is

$$C_1 = -\frac{\mu h_1}{4D_1} \overline{I}_1 \frac{\omega}{p_1} = -\frac{h_1 \overline{I}_1}{2} \sqrt{\frac{\omega\mu}{2D_1}}. \tag{17}$$

Similarly, the TM_0^z modal amplitude in the lower subregion C_2 can be found. From the energy point of view, total incident power of the incident TEM waves of current amplitude A_1 and A_2 is $|A_1|^2 + |A_2|^2$. The total reflected power carried by the TEM waves is $|B_1|^2 + |B_2|^2$. Meanwhile, the powers coupled into the radial waves are $|C_1|^2$ and $|C_2|^2$ in the upper and lower subregions, respectively.

VI. Numerical Results

Only numerical examples for a symmetrical structure with distance between two parallel plates $D_1 = D_2 = D$, via height $h_1 = h_2 = h$ and the transmission line radius $a_1 = a_2$ are considered here for the sake of simplicity, even though the present analysis can handle the asymmetrical structure without any difficulty. The parameters $\Gamma_{sc,i}$, $I_{sc,i}$, $T_{ant,i}$, $Y_{ant,i}$ and the via currents $I_{sc,i}(z)$, $I_{ant,i}(z)$ $(i = 1, 2)$ are the same in the both subregions. The subscript i is thus omitted for the sake of convenience.

Consider a TEM mode of unit amplitude incident from the line 1 ($A_1 = 1$) while line 2 is terminated with a match load ($A_2 = 0$). In this case, the transmission and reflection coefficients are given by

$$T = S_{21} = -T_{ant} \cdot I_{sc}/2Y_{ant}$$
$$\Gamma = S_{11} = \Gamma_{sc} + T. \tag{18}$$

Also, from (3) and (13), the current distribution on the upper and lower vias can be found to be

$$I_1(z) = I_{sc}(z) - \frac{I_{sc}(0)}{2Y_{ant}} \cdot I_{ant}(z)$$
$$I_2(z) = -\frac{I_{sc}(0)}{2Y_{ant}} \cdot I_{ant}(z). \tag{19}$$

Only a truncated section of the semi-infinitely long transmission line is actually included in the present analysis. It is verified that satisfactory results can be obtained if the section length L is chosen to be at least 1.5λ, just as the previous case without upper and lower conducting plates [12]. Numerical results in the following examples are obtained by choosing $L = 1.5\lambda$.

Consider a through hole via structure with $a_1 = a = 60\,\mu$m, $b = 180\,\mu$m, $h = 1.8$ mm, and $D = 3.6$ mm. Fig. 4 compares the results obtained by the present analysis and the FD-TD method, which are denoted by the solid and dashed curves, respectively. In FD-TD simulation, the circular wire and hole are replaced by square ones with size $2a$ and $2b$, respectively. The solution region is truncated into a rectangular box and is discretized using $80 \times 160\ p \times 120$ uniform orthogonal mesh, that is, 4.8 mm in width by 9.6 mm in length by 7.2 mm in height. The first-order Mur's absorbing boundary condition [21] is employed to approximate the outgoing waves at the truncated boundary. The incident wave is assumed to be a Gaussian pulse having a precomputed field distribution corresponding to the quasi-TEM mode along the transmission line. The discrepancy between these two sets of curves is reasonable since the structures considered in these two analyses are slightly different and probably even more, the absorbing boundary condition works not well for both the radial waves and TEM waves.

Fig. 5(a) and (b) shows the magnitude and phase of the reflection and transmission coefficients for the via structures with $h/a = 30$, $a_1/a = 1$, and D/h as the parameter. The solid curves standing for the limiting case $D \to \infty$ are obtained in the previous analysis [12]. The effects due to the presence of two outer plates can be depicted from the comparisons between the dashed and solid curves. The reflection coefficient is

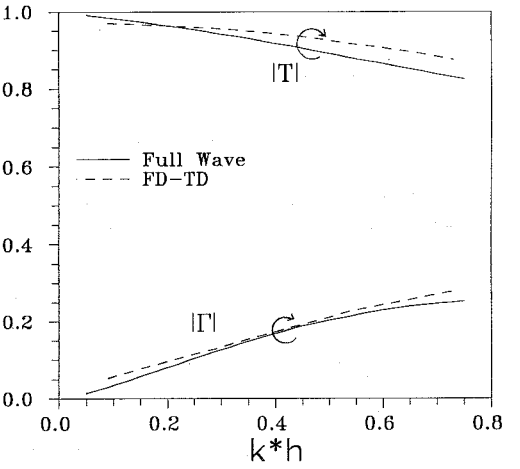

Fig. 4. Comparison between the results by present approach and FD-TD simulation, which are denoted by solid and dashed curves, respectively. The via structure has parameters $a_1 = a = 60\,\mu$m, $b = 180\,\mu$m, $h = 1.8$ mm, and $D = 3.6$ mm.

significantly reduced but the transmission coefficient remains almost the same. In other words, significant amount of energy is coupled to the radial waves. At low frequencies, the power loss is found to be a linear function of the frequency in the present case rather than a quadratic dependence if the two outer plates are absent. Using a frequency dependent resistance R to account for the power loss and referring to the circuit model shown in Fig. 1(b), the reflection coefficient at the quasistatic limit can be approximately given by

$$\Gamma \cong \frac{R}{Z_0} + j\omega\left(\frac{L_e}{Z_0} - C_e Z_0\right). \tag{20}$$

As the ratio D/h decreases, L_e will increase and Z_0 will decrease while C_e is relatively invariant. Consequently, the phase of Γ shown in Fig. 5(b) varies from $-90°$ to a positive value, i.e., the via behaves more inductively.

Fig. 5(c) shows the modal amplitudes C_1 and C_2 of the excited radial waves in the upper and lower subregions, respectively. Both C_1 and C_2 are almost the same at low frequencies as expected due to a nearly constant current distribution along the via. However, at substantially higher frequencies, the induced voltage V_0 and consequently the modal amplitude C_2 tends to be saturated. The modal amplitude C_1 shows reasonable increment which can be attributed to the associated grounded via structure in the upper subregion. Be worth mentioning, the total power carried by radial waves is found to be greater than the power loss $1-|\Gamma|^2-|T|^2$. The reason of this phenomenon is not quite sure right now. Probably, part of the radial waves are picked up by the transmission lines since the radial waves and the TEM waves are not orthogonal. Roughly speaking, the power carried by radial waves may become as high as 0.1 (10 db) even if the via height is as small as one fiftieth of a wavelength ($kh = 0.125$) for $D/h = 1.5$. Such occurrence clearly depicts that the vias between two parallel plates would cause severe coupling among themselves.

Fig. 6 presents the reflection coefficient versus the via height h while choosing different separations D and operating frequencies as the parameters. When the via height h is much

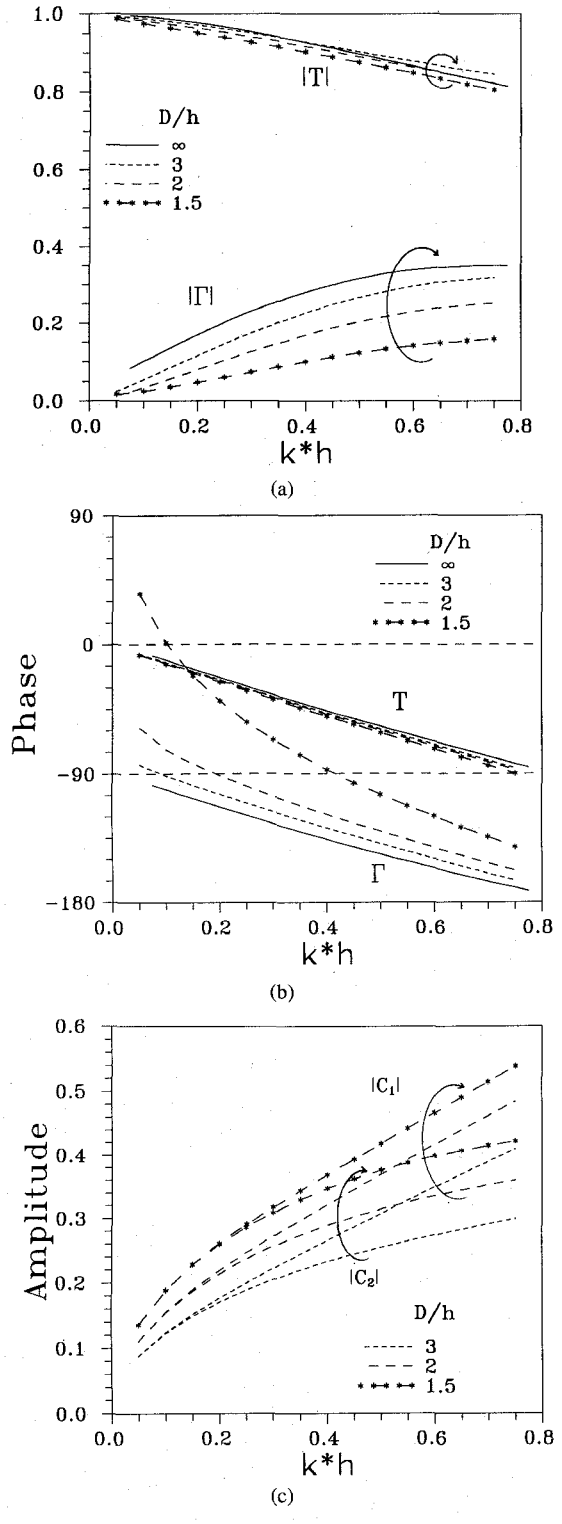

Fig. 5. Comparisons between this study and the previous research [12], which are denoted by dashed curves and solid curves, respectively. (a) Amplitude, (b) phase of the reflection and transmission coefficients, and (c) modal amplitude of the radial waves. The via structures have parameters $a_1/a = 1$ and $h/a_1 = 30$.

smaller than the separation D, the reflection slightly increases versus the via height. In the case of close parallel plates, say $D = 3$ mm, the via may exhibit resonance at a certain height where the reflection is a minimum. After that, the reflection significantly increases as the via height increases further. This occurrence can be explained by the equivalent circuit in Fig. 1(b). The via is dominantly capacitive if the via height is smaller that the resonant height. Since C_e remains almost a constant as via height h changes, the variation of the reflection coefficient is small. If the via height is larger than the resonant height, the via is dominantly inductive. The increase of reflection coefficient is significant due to a large dependence of L_e on the via height h.

Fig. 7 shows the ratio of the separation to the resonant height versus frequency for the via structure with $a_1 = a$ and h/a as the parameter. The curves are drawn by curve fitting the numerical results obtained at several different frequencies. It can be found that the optimal D/h ratio decreases as the frequency increases. These curves are helpful for designing a multi-layered packaging system with minimum reflection.

Although this paper mainly deals with a through hole via in multi-layered packaging, the analysis procedure yields important information regarding the two constitutive problems as a by-product. For example, the associated short circuit problem shown in Fig. 2(c) is usually encountered in shorted strip line. The normalized equivalent impedance $\overline{Z}_{sc}$ of the grounded via is given by

$$\overline{Z}_{sc} = (1 + \Gamma_{sc})/(1 - \Gamma_{sc}). \tag{21}$$

Fig. 8 shows the real and imaginary parts of $\overline{Z}_{sc}$ versus the frequency for the via structures with $a_1 = a$, $h/a_1 = 30$, and D/h as a parameter. Based on the quasistatic analysis, the grounded via is basically inductive at low frequencies and can be modeled by a lumped inductance L_e at low frequencies. Using the closed-form formula for the cases of $D/h = 3$ and 2 [22], the results denoted by symboled dashed straight curves ($\overline{Z}_{sc} = j\omega L_e Y_0$) are also shown for comparison sake. The agreement with the imaginary part of the full wave results is good at low frequencies. However, the quasistatic assumption fails to predict the nonnegligible real part of $\overline{Z}_{sc}$ which is contributed to the radial wave excited by the grounded via. Summing up, the equivalent impedance can be described by

$$\overline{Z}_{sc} Z_0 = \gamma kh \left(\frac{h}{D}\right)\eta + j\omega L_e \tag{22}$$

where the coefficient γ is empirically found to be about 1/5 and slightly increases versus the frequency.

Assuming the same via dimensions, Fig. 9 shows the input admittance Y_{ant} of the associated wire antenna shown in Fig. 2(b). At low frequencies, the imaginary part of Y_{ant} is positive in most of the cases, which depicts that the wire antenna is basically capacitive. In the case of very close parallel plates, say $D/h = 1.5$, the wire antenna is inductive at low frequencies and gradually becomes capacitive as frequency increases. The resonance frequency at which Y_{ant} is purely real is found to be nearly the same as that in Fig. 5(b). The real part of Y_{ant} does not tend to zero at the quasistatic limit due to the presence of the infinite transmission line and the radial waveguide. The value is observed to be slightly smaller than the characteristic admittance of the transmission line $Y_0 = 1/Z_0$ given in (12). The difference between the real part of Y_{ant} and the characteristic admittance Y_0 can be

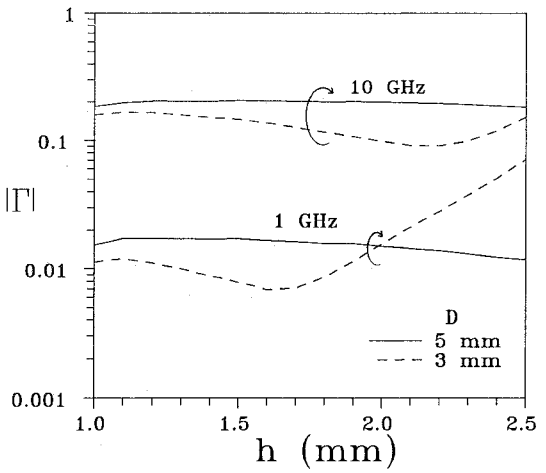

Fig. 6. Reflection coefficients at 1 and 10 GHz versus h for the via structures with $a_1 = a = 50\,\mu$m, and $D = 3$ or 5 mm.

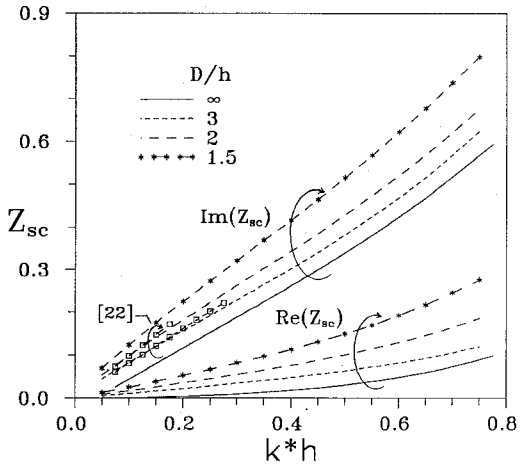

Fig. 8. Normalized impedance Z_{sc} of short circuit problem in Fig. 2(c) versus frequency for the via structures with $a_1/a = 1, h/a_1 = 30$, and D/h as a parameter.

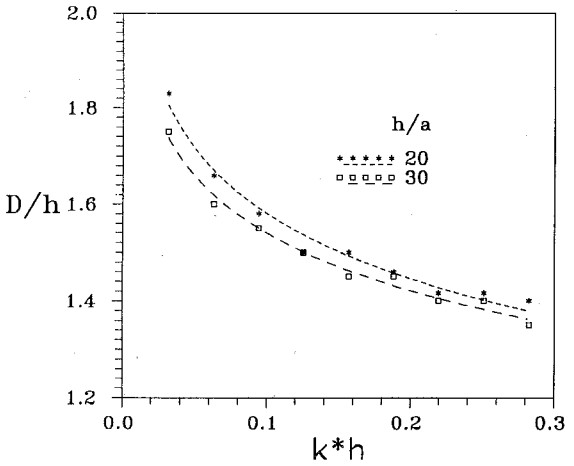

Fig. 7. The optimum ratio D/h of minimum reflection versus frequency for the via structures with $a_1 = a$ and h/a as a parameter.

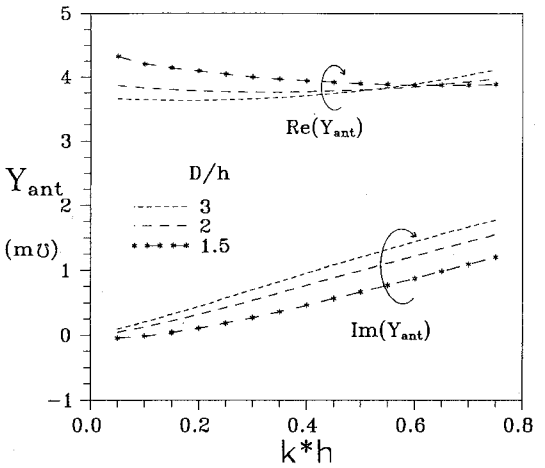

Fig. 9. Input admittance Y_{ant} of the wire antenna problem in Fig. 2(b) versus frequency for the via structures with $a_1/a = 1$, $h/a_1 = 30$, and D/h as a parameter.

defined as the energy transition Y_{tra}, which is proportional to the average power coupled to the radial waves.

VII. Conclusion

In this paper, a full wave approach was proposed for investigating the frequency dependent propagation characteristics of a through hole via in the multi-layered packaging environment. The problem was first decomposed into a short-circuit problem and a wire antenna problem, for each of which only the structure in a subregion required consideration. The current distribution on the via and a truncated section of transmission line was solved by the moment mothed and the scattering parameters were extracted by the matrix pencil method. The Green's function having an infinite series sum was evaluated by the help of the Poisson summation formula. The modal amplitude of the radial wave was obtained from the current distribution on the vertical through hole via.

The present analysis was compared with the previous study that deals with the same through hole via but without the upper and lower conducting plates. The results were found to be consistent as the parallel plates depart from each other. The simulation based on the FD-TD method also showed reasonable agreement with the results by the present analysis. Finally, numerical results were presented to investigate the propagation characteristics and the radial waves excitation versus frequency for the via structures with various geometrical parameters. Roughly speaking, the power carried by radial waves may become as high as 0.1 (10 db) even if the via height is only 0.02λ. By adjusting a suitable ratio of via height and separation of two plates, the via can achieve resonance and exhibit minimum reflection. Also presented were the equivalent impedances of both the associated grounded via and via antenna problems which include nonnegligible real parts to signify the presence of the excited radial waves. A quasistatic equivalent circuit model was given to explain the electrical performance associated with the via in multi-layered environment. The presented results justified that the equivalent circuit serves as a proper model for the via at low frequencies.

REFERENCES

[1] T. Dixon, "Multilayer ceramics: The key to high density interconnections," *Electronic Packaging Production,* pp. 76–82, Feb. 1983.

[2] A. J. Boldgett, Jr., "Microelectronic packaging," *Scientific American,* vol. 249, pp. 86–96, July 1983.

[3] A. E. Ruehli, "Equivalent circuit models for three-dimensional multiconductor systems," *IEEE Trans. Microwave Theory Tech.,* vol. MTT-22, pp. 216–221, May 1974.

[4] R. B. Wu and L. L. Wu, "Exploiting structure periodicity and symmetry in capacitance calculations for three-dimensional multiconductor systems," *IEEE Trans. Microwave Theory Tech.,* vol. MTT-36, pp. 1311–1318, Sept. 1988.

[5] R. B. Wu, C. N. Kuo, and K. K. Chang, "Inductance and resistance computations for three-dimensional multiconductor interconnection structures," *IEEE Trans. Microwave Theory Tech.,* vol. MTT-40, pp. 263–271, Feb. 1992.

[6] T. Y. Wang, R. F. Harrington, and J. R. Mautz, "The equivalent circuit of a via," *Trans. Soc. Comput. Simulation,* vol. 4, pp. 97–123, Apr. 1987.

[7] ——, "Quasistatic analysis of a microstrip via through a hole in a ground plane," *IEEE Trans. Microwave Theory Tech.,* vol. MTT-36, pp. 1008–1013, June 1988.

[8] ——, "The excess capacitance of a microstrip via in a dielectric substrate," *IEEE Trans. Computer-Aided Design,* vol. CAD-9, pp. 48–56, June 1990.

[9] P. Kok and D. De Zutter, "Capacitance of a circular symmetric model of a via hole including finite ground plane thickness," *IEEE Trans. Microwave Theory Tech.,* vol. MTT-39, pp. 1229–1234, July 1991.

[10] W. D. Becker, P. H. Harms, and R. Mittra, "Time-domain electromagnetic analysis of interconnects in a computer chip package," *IEEE Trans. Microwave Theory Tech.,* vol. MTT-40, pp. 2155–2163, Dec. 1992.

[11] R. Sorrentino, F. Alessandri, M. Mongiardo, G. Avitabile, and L. Roselli, "Full-wave modeling of via hole grounds in microstrip by three-dimensional mode matching technique," *IEEE Trans. Microwave Theory Tech.,* vol. MTT-40, pp. 2228–2234, Dec. 1992.

[12] S. G. Hsu and R. B. Wu, "Full wave characterization of a through hole via using the matrix-penciled moment method," *IEEE Trans. Microwave Theory Tech.,* vol. MTT-42, pp. 1540–1547, Aug. 1994.

[13] E. Zheng, R. F. Harrington, and J. R. Mautz, "Electromagnetic coupling through a wire-penetrated small aperture in an infinite conducting plane," *IEEE Trans. Electromagn. Compat.,* vol. EMC-35, pp. 295–300, May 1993.

[14] J. Fang, Y. Liu, Y. Chen, Z. Wu, and A. Agrawal, "Modeling of power noise in high speed digital electronics packaging," in *IEEE 2nd Topical Meet. Electrical Performance of Electronic Packaging,* Oct. 1993, pp. 206–208.

[15] J. M. Jong and V. K. Tripathi, "A model for parallel semi infinite conducting planes," in *IEEE 2nd Topical Meet. Electrical Performance of Electronic Packaging,* Oct. 1993, pp. 225–227.

[16] Q. Gu, Y. E. Yang, and M. A. Tassoudji, "Modeling and analysis of vias in multilayered integrated circuit," *IEEE Trans. Microwave Theory Tech.,* vol. MTT-41, pp. 206–214, Feb. 1993.

[17] K. K. Mei, "On the integral equations of thin wire antennas," *IEEE Trans. Antennas Propagat.,* vol. AP-13, pp. 374–378, May 1965.

[18] I. S. Gradshteyn and I. M. Ryzhik, *Table of Integrals, Series, and Products,* corrected and enlarged ed. Scripta Technica, 1980, p. 472.

[19] Y. B. Hua and T. K. Sarkar, "Generalized pencil-of-function method for extracting poles of an EM system from its transient response," *IEEE Trans. Antennas Propagat.,* vol. AP-37, pp. 229–234, Feb. 1989.

[20] C. A. Balanis, *Advanced Engineering Electromagnetics.* New York: Wiley, 1989, ch. 9, pp. 499–504.

[21] G. Mur, "Absorbing boundary conditions for the finite-difference approximation of the time-domain electromagnetic-field equations," *IEEE Trans. Electromagn. Compat.,* vol. EMC-23, pp. 377–382, Nov. 1981.

[22] R. B. Wu, "Electrical analysis of wirings in thin-film packaging (I)," Res. Rep. of National Science Council, R.O.C., pp. 102–103, July 1993.

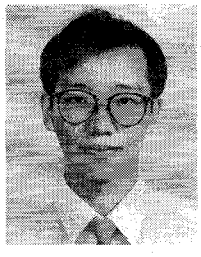

Show-Gwo Hsu was born in Chunghwa, Taiwan, R. O. C., in 1966. He graduated from the National Taipei Institute of Technology, Taipei, Taiwan, in 1986, and received the M.S. degree from the National Taiwan University, Taipei, Taiwan, in 1991. Currently, he is pursuing the Ph.D. degree in electrical engineering at the National Taiwan University.

His research interests include electromagnetic theory, antenna theory and measurement, and electronic packaging analysis.

Ruey-Beei Wu was born in Tainan, Taiwan, R. O. C., in 1957. He received the B.S.E.E. and Ph.D. degrees from National Taiwan University, Taipei, Taiwan, in 1979 and 1985, respectively.

In 1982, he joined the faculty of the Department of Electrical Engineering, National Taiwan University, where he is now a professor. From March 1986 to February 1987, he was a visiting scientist in the IBM General Technology Division laboratory, East Fishkill Facility, Hopewell Junction, NY. He is currently visiting the Electrical Engineering Department, University of California in Los Angeles. He works primarily on the applications of numerical methods to electromagnetic field problems. He has been engaged in researches on dielectric waveguides, optical fibers, wave scattering of anisotropic objects and composite materials, edge slot antennas, transmission line discontinuities, and interconnection modeling for computer packaging.